Clin Orthop Relat Res
DOI 10.1007/s11999-012-2366-8

Clinical Orthopaedics and Related Research®
A Publication of The Association of Bone and Joint Surgeons®

ORTHOPAEDIC CASE OF THE MONTH

A 16-year-old Boy with Multifocal, Painless Osseous Lesions

Ellen M. Dean MD, James C. Wittig MD, Camilo Vilalobos MD, Roberto A. Garcia MD

Received: 16 October 2011 / Accepted: 12 April 2012

History and Physical Examination

A 16-year-old boy presented with left wrist pain of 8 months' duration. There was a remote history of a hyperextension injury to the wrist while weight lifting. He denied all constitutional symptoms. He had taken NSAIDs intermittently with no resolution of symptoms. He was an otherwise healthy adolescent with no significant medical history. His family history was noncontributory. The patient had been seen by an orthopaedist who suspected triangular fibrocartilage complex (TFCC) tear and ordered MRI without contrast. The MRI showed several well-defined intramedullary lesions in the distal radius and carpal bones that were suggestive of leukemia. The orthopaedist then obtained a bone marrow biopsy which showed normocellular marrow with trilineage hematopoiesis and no evidence of acute leukemia. The patient then was referred for orthopaedic oncology evaluation for additional workup of the lesions seen on the MR images.

On examination, the patient was a healthy-appearing teenager with stable vital signs. Focused examination of the wrist showed tenderness to palpation at the TFCC. Ulnar deviation of the wrist provoked ulnar-sided wrist pain. There were no palpable masses, deformities, swelling, or bony tenderness. He had no lymphadenopathy. The rest of his physical examination was normal.

Laboratory examinations showed a slightly increased white blood cell count of 11.0 (10^3/L) with a differential of 61% neutrophils, 28% lymphocytes, 8.7% monocytes, 1.4% eosinophils, and 0.3% basophils. Erythrocyte sedimentation rate was increased at 35 mm/hour. Total protein electrophoresis was increased in the α1-globulin region to 0.56 g/dL (normal, 0.19–0.46 g/dL) and in the α2-globulin to 1.19 g/dL (normal, 0.48–1.05 g/dL).

Plain radiographs of the wrist showed no abnormalities. Based on these imaging studies, further workup, including contrast enhanced MRI (Fig. 1), CT scan (Fig. 2) of the left wrist, and a whole-body bone scan (Fig. 3), were performed.

Based on the history, physical examination, laboratory studies, and imaging studies, what is the differential diagnosis at this point?

Each author certifies that he or she, or a member of his or her immediate family, has no commercial associations (eg, consultancies, stock ownership, equity interest, patent/licensing arrangements, etc) that might pose a conflict of interest in connection with the submitted article.
All ICMJE Conflict of Interest Forms for authors and *Clinical Orthopaedics and Related Research* editors and board members are on file with the publication and can be viewed on request.
Each author certifies that his or her institution approved the reporting of this case report, that all investigations were conducted in conformity with ethical principles of research, and that informed consent for participation in the study was obtained.
This work was performed at The Mount Sinai Hospital/Mount Sinai School of Medicine Department of Orthopaedic Surgery.

E. M. Dean (✉)
Department of Orthopaedic Surgery, Seton Hall University/St. Joseph's Regional Medical Center, 703 Main Street, Paterson, NJ 07503, USA
e-mail: ellen.dean80@gmail.com

J. C. Wittig, C. Vilalobos
Department of Orthopaedic Surgery, The Mount Sinai Hospital/ Mount Sinai School of Medicine, New York, NY, USA

R. A. Garcia
Department of Pathology, The Mount Sinai Hospital, New York, NY, USA

Published online: 28 April 2012

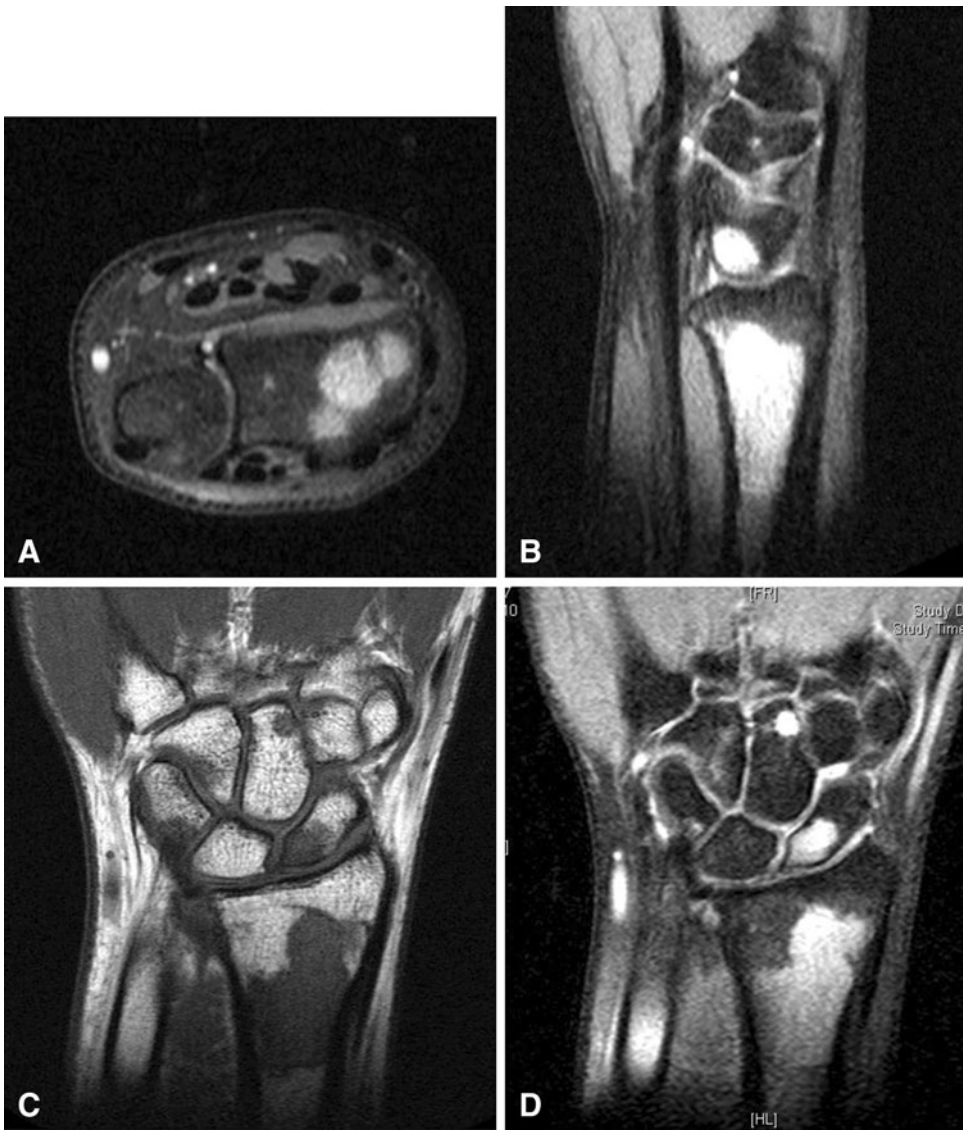

Fig. 1A–D (**A**) Axial and (**B**) sagittal T2-weighted MR images of the distal radius show hyperintense lesions in the distal radius and lunate. The lesions were of intermediate signal on (**C**) the coronal T1-weighted MR image and hyperintense on (**D**) the coronal T2-weighted fast spin echo MR image.

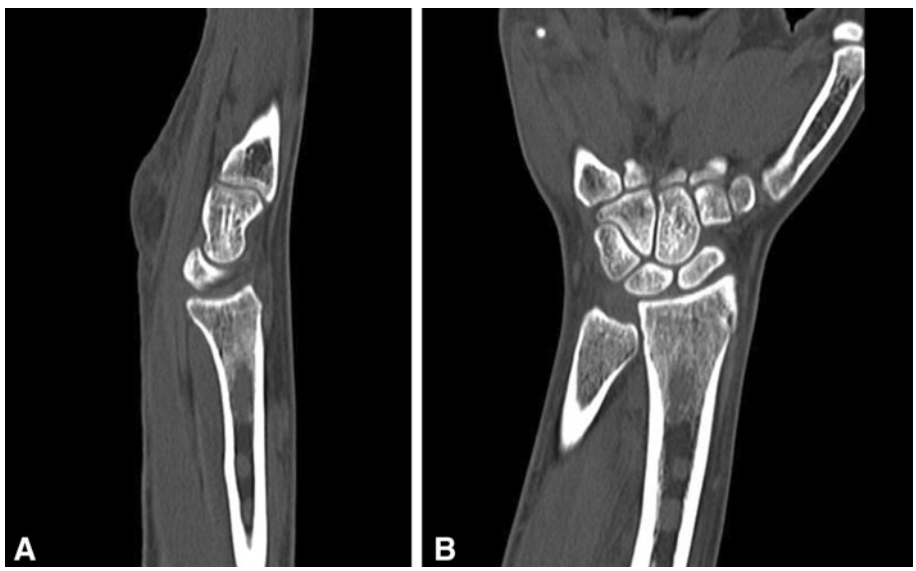

Fig. 2A–B (**A**) Sagittal and (**B**) coronal reconstructions of a CT scan of the wrist show multiple permeative lesions in the distal radius that are not as well-defined as those seen on MRI.

Imaging Interpretation

MRI of the left wrist using multiplanar and multisequence techniques revealed several well-defined intramedullary lesions in the distal radius and carpal bones (scaphoid, capitate, triquetrum, and hamate) (Fig. 1A–B). The lesions were of intermediate signal intensity on T1-weighted images (Fig. 1C) and hyperintense signal intensity on T2-weighted images (Fig. 1D). The lesion in the distal radius was located in the metaphysis, just abutting the physeal scar. There was no cortical destruction or associated soft tissue mass. CT scan of the left wrist (Fig. 2) showed multiple permeative lesions in the distal radius. There was no mineralization in these lesions.

A whole-body bone scan (Fig. 3) was performed, which showed intense tracer uptake in the left distal radius and carpal bones corresponding to the lytic lesions seen on MRI. In addition, there was increased asymmetric tracer uptake in the right distal tibia, right carpus, right frontal aspect of the skull, and proximal tibias.

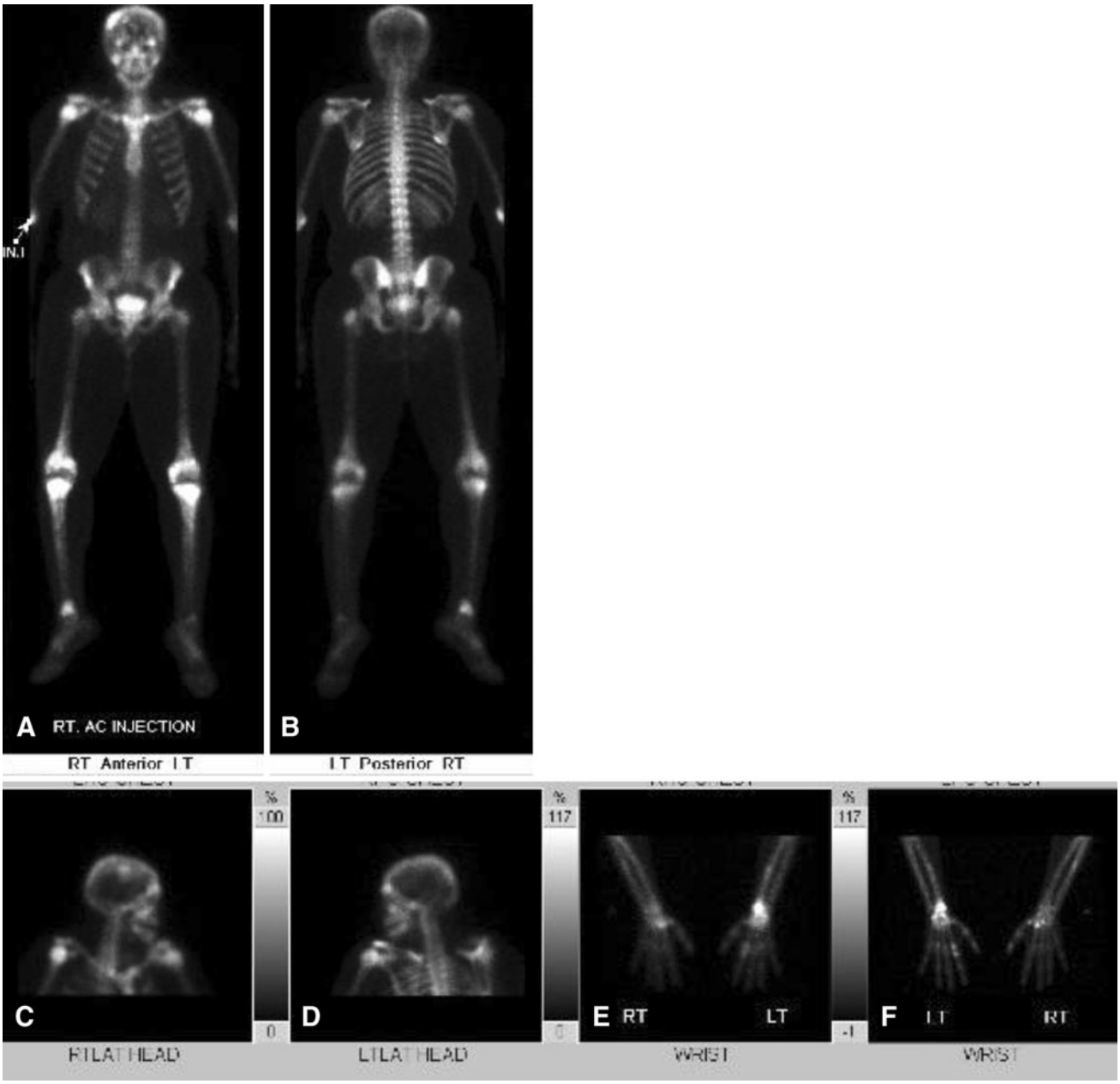

Fig. 3A–F (**A**) Anterior and (**B**) posterior whole-body bone scans, (**C**) anterior and (**D**) posterior bone scans of the head, and (**E**) anterior and (**F**) posterior bone scans of the hands reveal multiple areas of intense tracer uptake, including the left distal radius and carpus, right distal tibia, right carpus, right frontal bone, and bilateral proximal tibias.

Subsequent MRI of the right ankle lesion was performed with and without contrast. This showed multifocal areas of marrow replacement involving the distal tibial diaphysis, metaphysis, and epiphysis, similar to that observed in the distal radius. The lesions were well demarcated and of diminished signal intensity on T1-weighted images and hyperintense on T2-weighted images and STIR sequences. There was diffuse enhancement of the lesions on the postcontrast images. Radiographs of the distal tibia also were normal.

Differential Diagnosis

Langerhans cell histiocytosis
Chronic recurrent multifocal osteomyelitis
Lysosomal storage disease
Histiocytic disease of bone (Rosai-Dorfman disease)
Polyostotic fibrous dysplasia (McCune-Albright syndrome)
Lymphoma
Metastases

An open biopsy of the lesion in the left distal radius was performed. Several cores of tissue and blood via aspiration were sent for analysis (Fig. 4).

Based on the history, physical examination, laboratory studies, imaging studies, and histologic picture, what is the diagnosis and how should the patient be treated?

Histology Interpretation

The biopsy specimen showed infiltration of the intertrabecular spaces by a population of large histiocytes (Fig. 4A) with abundant pale vacuolated cytoplasm, round to oval nuclei with fine chromatin, and small nucleoli (Fig. 4B). No atypia or necrosis was seen. There was conspicuous lymphophagocytosis (emperipolesis) and erythrophagocytosis. Scattered plasma cells and eosinophils also were present. Immunohistochemical stains revealed the large histiocytes were positive for S-100 protein (Fig. 4C), CD68, CD163, and CD45. Stains for CD1A, CD3, CD20, CD30, and HMB-45 were negative.

Diagnosis

Extranodal, multifocal Rosai-Dorfman disease.

Discussion and Treatment

The final diagnosis of extranodal Rosai-Dorfman disease (RDD) was made based on the suspicion of a multifocal

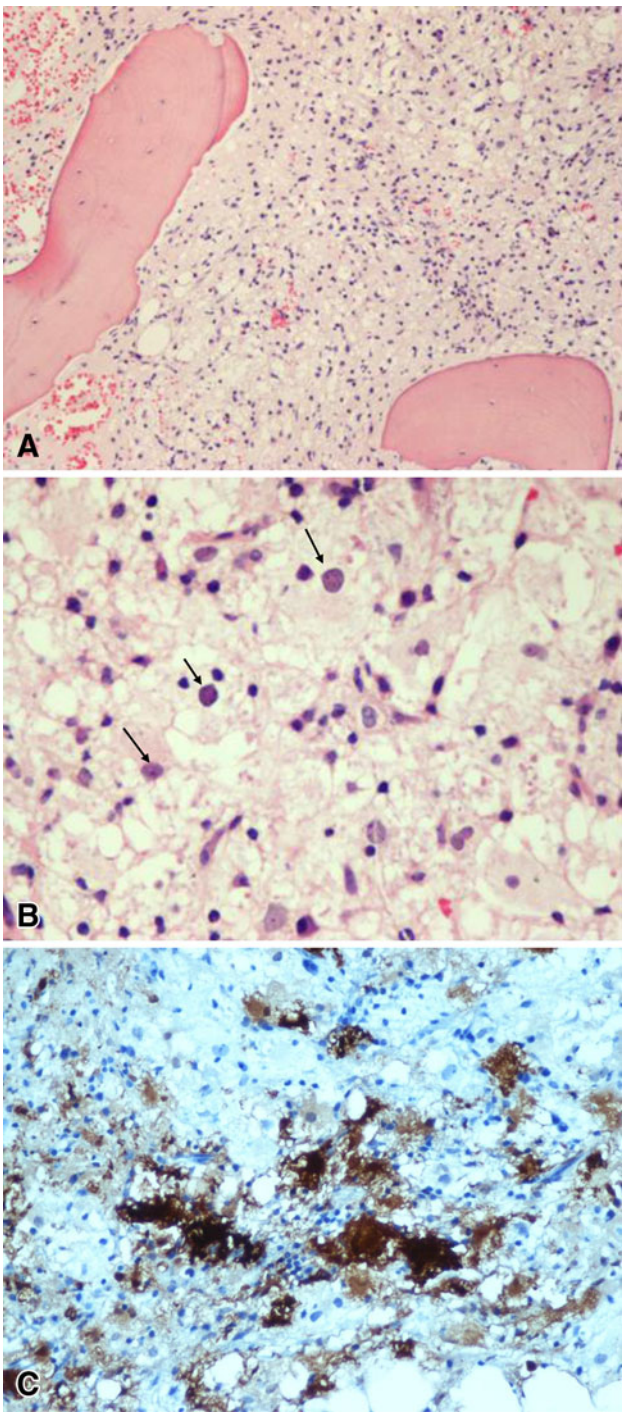

Fig. 4A–C (**A**) A photomicrograph shows marrow replacement by a population of large histiocytes with abundant pale cytoplasm admixed with chronic inflammatory cells (Stain, hematoxylin and eosin; original magnification, ×10). (**B**) A photomicrograph shows large histiocytes with vacuolated pale cytoplasm, round to ovoid nuclei, fine chromatin, and small nucleoli with lymphophagocytosis (emperipolesis, arrows) (Stain, hematoxylin and eosin; original magnification, ×40). (**C**) A photomicrograph of immunohistochemical staining showed that the large histiocytes were positive for the S-100 protein.

osseous disorder observed on imaging studies and confirmed with the histology and immunochemical staining. The ulnar-sided wrist pain that our patient experienced was the result of an injury to the TFCC. The lesions seen on imaging studies were incidental findings.

The differential diagnosis included Langerhans cell histiocytosis (LCH), chronic recurrent multifocal osteomyelitis (CRMO), polyostotic fibrous dysplasia, lysosomal storage disease, leukemia, and primary lymphoma of bone. All of these differential diagnoses can have variable presentations clinically and radiographically, which adds to the difficulty of making this diagnosis. To make a definitive diagnosis of RDD or any of these other entities, a pathologic diagnosis often is needed. LCH is the most closely related condition to RDD based on the radiographic findings. However, LCH differs from RDD based on the histologic presentation. LCH usually exhibits many eosinophils and histiocytes with hyperlobulated, convoluted nuclei. Immunohistochemical staining is always CD1a and langerin positive in LCH. In addition, the presence of Birbeck granules observed on electron microscopy would aid in differentiating the two disorders [11, 12]. CRMO is a multifocal idiopathic inflammatory disease of bone. However, it can exhibit an intense lamellar periosteal reaction on plain radiographs [15]. CRMO will respond to NSAIDS as this is the preferred treatment [14]. Polyostotic fibrous dysplasia usually is accompanied by precocious puberty [17]. The radiographic manifestations of the bone lesions take on a ground-glass appearance with cortical expansion [17]. In lysosomal storage diseases, such as Gaucher disease or mucopolysaccharidoses, the radiographic appearance is that of expansion of the metaphysis leading to an Erlenmeyer flask deformity. Primary lymphomas of bone rarely can present with multiple destructive bone lesions [8, 16]. The lymphomas that affect children and adolescents are typically the B-cell non-Hodgkin's variety that may be accompanied by systemic B symptoms (fever, weight loss, night sweats) [8, 16]. In addition, bone metastases always must remain in the differential diagnosis for a child with multiple skeletal lesions. Most commonly, neuroblastoma is the primary tumor that will metastasize to the bone in children [6, 7]. However, this feature also can be seen with Ewing's sarcoma, osteosarcoma, and renal tumors [6, 7].

RDD is a rare disorder of benign histiocytic proliferation of unknown origin. It was first described in 1969 by the pathologists Juan Rosai and Ronald Dorfman as a distinct clinicopathologic entity [20]. The classic presentation is characterized by painless bilateral cervical lymphadenopathy, fever, leukocytosis, increased erythrocyte sedimentation rate, and hypergammaglobulinemia [2, 7, 10, 20]. In 43% of patients, there is combined multifocal and multisystem involvement along with nodal involvement [1, 7, 19]. There can be isolated extranodal involvement in a reported 23% of patients, most commonly in the head and neck [22]. Osseous involvement with nodal disease occurs rarely in less than 8% of patients [4, 5]. Osseous involvement without lymphadenopathy is exceedingly rare, accounting for only 2% of all reported cases [5, 21].

Although the etiology of RDD is unknown, it is thought to be an immunologic disorder. Although it has not been proven, it has been postulated RDD is a response to an infectious agent with subsequent lymph node proliferation [5, 7]. This in turn leads to an immunosuppressed state as proliferations of histiocytes phagocytose active lymphocytes.

RDD is most commonly seen in the first or second decade of life. However, it can be seen in any age group, with the oldest reported patient being diagnosed at 74 years of age [2, 9]. A slight predilection for males has been detected and it has been observed in a slightly higher incidence in people of African descent [10, 19].

The natural history and symptoms depend on the site(s) involved by the disease. Symptoms typically are related to compression caused by massive painless lymphadenopathy [2, 7, 10]. In addition, organ dysfunction can be seen when extranodal sites are involved. These extranodal sites are most commonly the nasal cavity and paranasal sinuses [22]. However, virtually all extranodal sites can be involved, including skin, soft tissue, bone, central nervous system, orbits, kidney, liver, and heart [10, 13]. When only bone is involved, patients usually report having pain at the involved site. If there are skull lesions, headaches and seizures can be presenting symptoms. However, the radiographic lesions of osseous RDD are often incidental findings [3]. The clinical course of RDD is typically self-limited. Greater than 70% of patients have spontaneous resolution of symptoms [7, 19]. In a small subset of patients, there may be relapsing and remitting symptoms. The condition takes on a chronic and stable state in the majority of patients. In general, RDD has a favorable prognosis. The prognosis tends to worsen as the number of nodal sites increases and extranodal symptoms worsen [10]. Mortality is exceedingly rare but has been seen with disseminated nodal disease, presence of disease at rare extranodal sites, and when in conjunction with other systemic immunologic disorders [13].

The best treatment of RDD is unknown owing to its low incidence. Most patients require observation alone as the disease tends to spontaneously resolve. Patients with recurrent symptoms, particularly rapid lymph node swelling and fevers, have been treated successfully with steroids [10, 19]. In addition, response to chemotherapy (methotrexate and vinblastine) has been documented for patients whose disease is resistant to steroids. Radiation also has been used as adjunctive therapy, but with doses of 20 to

30 Gy [19]. Surgical debulking is indicated for compressive symptoms not responsive to steroid treatment.

We did not institute treatment in our patient but are following him at 4- to 6-month intervals with serial laboratory studies (including complete blood counts, erythrocyte sedimentation rates, C-reactive proteins, and total protein electrophoresis) and whole-body diffusion-weighted MRI [18]. We will use this imaging study to assess the activity and distribution of his lesions without the need for intravenous contrast or radiation [18]. This case emphasizes the need to keep in mind a wide differential diagnosis, including rare entities, when it comes to multicentric painless bony lesions. This case also highlights the need to further investigate lesions that appear on MR images but are not seen on a plain radiograph. Ultimately, to diagnose RDD, a histologic analysis must be performed that shows emperipolesis and histiocytes that stain positive for S-100.

Acknowledgment We thank Juan Rosai MD, for reviewing the histology slides and confirming the diagnosis.

References

1. Abdelwahab IF, Klein MJ, Springfield DS, Hermann G. A solitary lesion of talus with mixed sclerotic and lytic changes: Rosai-Dorfman disease of 25 years' duration. *Skeletal Radiol*. 2004:33:230–233.
2. Agarwal A, Pathak S, Gujral S. Sinus histiocytosis with massive lymphadenopathy: a review of seven cases. *Indian J Pathol Microbiol*. 2006:49:509–515.
3. Bachmann KR, Dragoescu EA, Foster WC. Extranodal Rosai-Dorfman disease presenting as an incidental bone tumor: a case report. *Am J Orthop (Belle Mead NJ)*. 2010:11;E123–E125.
4. Chopra D, Svensson WE, Forouhi P, Poole S. A rare case of extranodal Rosai-Dorfman disease. *Br J Radiol.* 2006;79:e117–e119.
5. Demicco EG, Rosenberg AE, Bjornsson J, Ryback LD, Unni KK, Nielsen GP. Primary Rosai-Dorfman disease of bone: a clinicopathologic study of 15 cases. *Am J Surg Pathol*. 2010;34;1324–1333.
6. Deutsch M, Tersak J. Radiotherapy for symptomatic metastases to bone in children. *Am J Clin Oncol*. 2004;27:128–131.
7. Foucar E, Rosai J, Dorfman RF. Sinus histiocytosis with massive lymphadenopathy (Rosai-Dorfman disease): review of the entity. *Semin Diagn Pathol*. 1990;7:19–73.
8. Gebert C, Hardes J, Ahrens H, Buerger H, Winkelmann W, Gosheger G. Primary multifocal osseous Hodgkin disease: a case report and review of the literature. *J Cancer Res Clin Oncol.* 2005;131:163–168.
9. George J, Stacy G, Peabody T, Montag A. Rosai-Dorfman disease manifesting as a solitary lesion of the radius in a 41-year-old woman. *Skeletal Radiol.* 2003;32:236–239.
10. Gupta P, Babyn P. Sinus histiocytosis with massive lymphadenopathy (Rosai-Dorfman disease): a clinicoradiological profile of three cases including two with skeletal disease. *Pediatr Radiol*. 2008;38:721–728; quiz 821–822.
11. Hindman BW, Thomas RD, Young LW, Yu L. Langerhans cell histiocytosis: unusual skeletal manifestations observed in thirty-four cases. *Skeletal Radiol*. 1998;27:177–181.
12. Hoover KB, Rosenthal DI, Mankin H. Langerhans cell histiocytosis. *Skeletal Radiol*. 2007:36:95–104.
13. Huang Q, Chang K, Weiss L. Extranodal Rosai-Dorfman disease involving bone marrow. *Am J Surg Pathol*. 2006;30:1189–1192.
14. Jurik AG. Chronic recurrent multifocal osteomyelitis. *Semin Musculoskelet Radiol.* 2004;8:243–253.
15. Khanna G, Sato TS, Ferguson P. Imaging of chronic recurrent multifocal osteomyelitis. *Radiographics*. 2009;29:1159–1177.
16. Langley CR, Garrett SJ, Urand J, Kohler J, Clarke NM. Primary multifocal osseous Hodgkin's lymphoma. *World J Surg Oncol.* 2008;6:34–40.
17. Parekh SG, Donthineni-Rao R, Ricchetti E, Lackman RD. Fibrous dysplasia. *J Am Acad Orthop Surg.* 2004;12:305–313.
18. Rittner RE, Baumann U, Laenger F, Hartung D, Rosenthal H, Heuper K. Whole-body diffusion-weighted MRI in a case of Rosai-Dorfman disease with exclusive multifocal involvement. *Skeletal Radiol.* 2011 Dec 3 [Epub ahead of print].
19. Rodriguez-Galindo C, Helton KJ, Sanchez ND, Rieman M, Jeng M, Wang W. Extranodal Rosai-Dorfman disease in children. *J Pediatr Hematol Oncol*. 2004;26:19–24.
20. Rosai J, Dorfman RF. Sinus histiocytosis with massive lymphadenopathy: a newly recognized benign clinicopathological entity. *Arch Pathol*. 1969:87:63–70.
21. Sundaram C, Uppin Shantveer G, Chandrashekar P, Prasad VB, Umadevi M. Multifocal osseous involvement as the sole manifestation of Rosai-Dorfman disease. *Skeletal Radiol.* 2005:34:658–664.
22. Yoon AJ, Parisien M, Feldman F, Young-In-Lee F. Extranodal Rosai-Dorfman disease of bone, subcutaneous tissue and paranasal sinus mucosa with a review of its pathogenesis. *Skeletal Radiol*. 2005:34;653–657.